journal

J. Am. Ceram. Soc., 89 [2] 754–758 (2006)
DOI: 10.1111/j.1551-2916.2005.00778.x

Biaxial Strength of a $ZrO_2/(Ni+Al_2O_3)$ Nanocomposite

Wei-Hsing Tuan,*,† Shi-Ming Liu, and Chan-Ju Ho

Department of Materials Science and Engineering, National Taiwan University, Taipei, Taiwan

Tsong-Jen Yang

Department of Materials Science, Fa-Chia University, Taichung, Taiwan

Previous studies demonstrated that the strength of zirconia (ZrO_2) could be enhanced or reduced by respectively adding micrometer-sized alumina (Al_2O_3) or nickel (Ni) particles. In the present study, 5 vol% micrometer-sized Al_2O_3 particles and 1 vol% nanometer-sized Ni particles are incorporated into the ZrO_2 matrix, which is subsequently densified by pressureless sintering. The biaxial strength of the $ZrO_2/(Ni+Al_2O_3)$ nanocomposite is nearly double that of the monolithic ZrO_2. The increase in strength correlated with a reduction in the critical flaw size and not with any change in toughness, which may be a result of grain boundary strengthening.

I. Introduction

The strength and toughness of zirconia (ZrO_2) are the best among various ceramics at room temperature. Hence, ZrO_2 has been chosen as a material for kitchen accessories, such as scissors, knives, etc. Furthermore, the surface finish of ZrO_2 component after suitable machining can be very smooth. Zirconia has thus been used as ferrule material for optical connectors. The tetragonal phase of ZrO_2 is not stable enough for long-term application under ambient conditions[1]; however, the addition of alumina (Al_2O_3) particles to ZrO_2 is one of the effective methods of inhibiting low-temperature degradations.[2] Furthermore, the addition of micrometer-sized Al_2O_3 particles may give rise to an extra strength enhancement.[3]

ZrO_2-based ceramics exhibit many other interesting properties. For example, oxygen vacancies transport quickly through ZrO_2, and thus it can be used as electrolyte for oxygen sensors.[4] By exploiting the high electrical conductivity of metallic Ni, ZrO_2/Ni composite has been used as the anode material for solid oxide fuel cells (SOFC).[5] The elastic modulus and thermal expansion coefficient (TEC) of ZrO_2 are close to those of Ni; the ZrO_2–Ni system thus has the potential to act as a model composite system. Nevertheless, apart from the application for SOFC, studies on the mechanical properties of ZrO_2/Ni composites are lacking.[6] The limited data on the mechanical properties of ZrO_2/Ni composites indicate that addition of 20–40 vol% micrometer-sized Ni particles would decrease the strength of ZrO_2.[6] In contrast, a recent study demonstrated that the addition of 1–2 vol% nanometer-sized Ni particles could enhance the strength of ZrO_2 by 20%.[7] Furthermore, the ZrO_2/Ni nanocomposite exhibits ferromagnetic characteristics that provide the possibility of remote sensing applications. ZrO_2 with an amount of Ni additive close to its percolation threshold exhibits a high relative permittivity,[8] and therefore, such a composite has been proposed for actuating applications. Nevertheless, mechanical integrity of the composite is essential for any functional application.

In the present study, both micrometer-sized Al_2O_3 and nanometer-sized Ni particles are added into a ZrO_2 matrix. The mechanical properties of the $ZrO_2/(Ni+Al_2O_3)$ nanocomposite are determined. The magnetic and dielectric properties of the nanocomposite are also determined.

II. Experimental Procedures

Yttrium-doped ZrO_2 powder (TZ-3Y, ZrO_2+3 mol% Y_2O_3, $d_{50} = 230$ nm, Tosoh Co., Tokyo, Japan) was mixed with 5 vol% Al_2O_3 (TM-DAR, $d_{50} = 210$ nm, Taimei Chem. Co. Ltd., Tokyo, Japan) powder by ball milling in de-ionized water for 24 h. Ammonia drops were added to the mixed powder slurry to achieve a pH value of 9.2. A separate solution of Ni nitrate ($Ni(NO_3)_2 \cdot 6H_2O$, Showa Chem. Co., Tokyo, Japan) with the same pH value was also prepared. The mixed powder slurry was poured into the Ni nitrate solution; the whole mixture was stirred for 30 min. The amount of Ni in the slurry was 5 vol% of the ZrO_2-based powder mixtures, provided that all Ni ions were adsorbed onto the surface of the ceramic particles. The Ni-coated powder mixture was filtered, washed, and dried. The mixture was then reduced in pure hydrogen at 550°C for 1 h, followed by ball milling in ethyl alcohol for 24 h with ZrO_2 grinding media. Reference ZrO_2, ZrO_2/Al_2O_3, and ZrO_2/Ni specimens were also prepared with the same technique for comparison purpose.

The amount of Ni in the powder mixture was determined by inductive coupled plasma-atomic emission spectroscopy (ICP-AES, 3000DV, Perkin–Elmer, Optima, Boston, MA). Green compacts with a diameter of 25.4 mm and a thickness of 5 mm were formed by uniaxial pressing at 30 MPa. The compacts were then sintered within a covered graphite mold at 1600°C for 1 h; they were covered with graphite powder in the mold. A reducing atmosphere, carbon monoxide mainly, was generated during sintering. The heating and cooling rates were 5°C/min.

Phase identification was performed by X-ray diffractometry (XRD) with CuKα radiation. Two scanning rates were used: 0.05°/s for phase identification and 0.002°/s for quantitative analyses. The final densities of the specimens were determined by the Archimedes method. Assuming that the solubility between the materials used in the present study was low; the relative densities of the composites were estimated from the theoretical densities of ZrO_2, Al_2O_3, and Ni, which are 6.05, 3.98 and 8.90 g/cm^3, respectively. The microstructure of the specimens was observed by scanning electron microscopy (SEM). Polished surfaces of the specimens were prepared by grinding and polishing with a 3 μm diamond paste and a 0.05 μm silica suspension. A thermochemical technique[9] was used in the

M. Harmer—contributing editor

Manuscript No. 20553. Received May 10, 2005; approved September 15, 2005.
Supported by the National Science Council, Taiwan, through the contract no. NSC93-2216-E-002-016.
*Member, American Ceramic Society.
†Author to whom correspondence should be addressed. e-mail: tuan@ccms.ntu.edu.tw

present study to determine the grain boundaries of the composites. The polished specimens were subjected to chemical etching with a solution of 0.8*N* orthophosphoric acid and 0.5*N* nitric acid (3:1) for 4–5 min, followed by thermal etching at 1250°C for 30 min. The line intercept technique was used to determine the size of the matrix ZrO_2 grains; more than 200 grains were counted. The size of Ni inclusions in the fired composites was estimated from the XRD patterns by the Scherrer formula.[10] The amount of *m*-phase ZrO_2 was estimated using the formula proposed by Evans *et al.*[11]

In preparation for mechanical testing, the sintered specimen disks were first ground with a 325 grit resin-bonded diamond wheel at depths of 5 μm/pass. The elastic modulus of the specimens was determined with an ultrasonic technique at 5 MHz (pulse receiver 5055PR and oscilloscope 9345CM, LeCroy Co., New York, NY). The strength of the disks was determined by a biaxial flexure technique[9] in a universal testing machine (MTS 810, MTS Co., Eden Prairie, MN). A one-ball-on-three-balls jig was used; the loading rate was 0.5 mm/min. Four disks of each composition were used for the strength measurement. The fracture toughness was determined by an indentation technique at a load of 196 N. The relationship proposed by Lawn *et al.*[12] was used to calculate the toughness from the indentation data. The magnetization curves were obtained by a SQUID magnetometer (MPMS7, Quantum Design Co., San Diego, CA). The dielectric constant was measured by an LCR meter (2330A, NF Electronic Instrument Co., Yokohama, Japan) at an excitation voltage of $\pm 1V$ at 1 kHz.

III. Results

The ICP analysis showed that the amount of Ni in the ZrO_2/Ni and ZrO_2/(Ni+Al_2O_3) powder mixtures was much less than the amount originally added to the slurry (see Table I). This indicates that only part of the added Ni ions is adsorbed onto the surface of the ceramic particles. Most Ni ions are filtered and removed during the solution-coating stage. Figure 1 shows the XRD patterns of the specimens after sintering and surface grinding. A small amount of m-phase ZrO_2 was found on the ground surface. At faster scanning rates, XRD analysis showed neither Al_2O_3 nor Ni peaks. However, the (111) peak of Ni was detected at a slower scanning rate. The size of Ni inclusions can thus be estimated by measuring the full-peak width at half-maximum intensity (FWHM).[10] The size of Ni particles in the starting powder mixture was 20 nm. The Ni inclusions remained small after sintering: less than 40 nm (see Table I).

The densities of the ZrO_2/Ni and ZrO_2/(Ni+Al_2O_3) specimens were higher than 98%, indicating that dense Ni-containing nanocomposites can be prepared by pressureless sintering. Figure 2 shows the typical micrographs of the specimens. The

Table I. Composition of Specimens Investigated in the Present Study and Their Microstructural Features

	Ni (vol%)	Al_2O_3 (vol%)	Relative density (%)	ZrO_2 grains (μm)	Ni inclusion (nm)
ZrO_2	—	—	97.5	0.79	—
ZrO_2/Al_2O_3	—	5.0	97.9	0.89	—
ZrO_2/Ni	0.9	—	100	1.4	37
ZrO_2/(Ni+Al_2O_3)	0.7	5.2	98.3	1.2	35

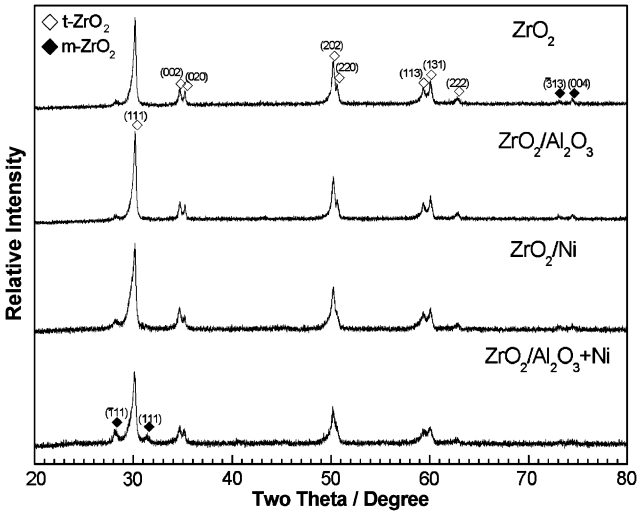

Fig. 1. X-ray diffractometry patterns of specimens after pressureless sintering and surface grinding.

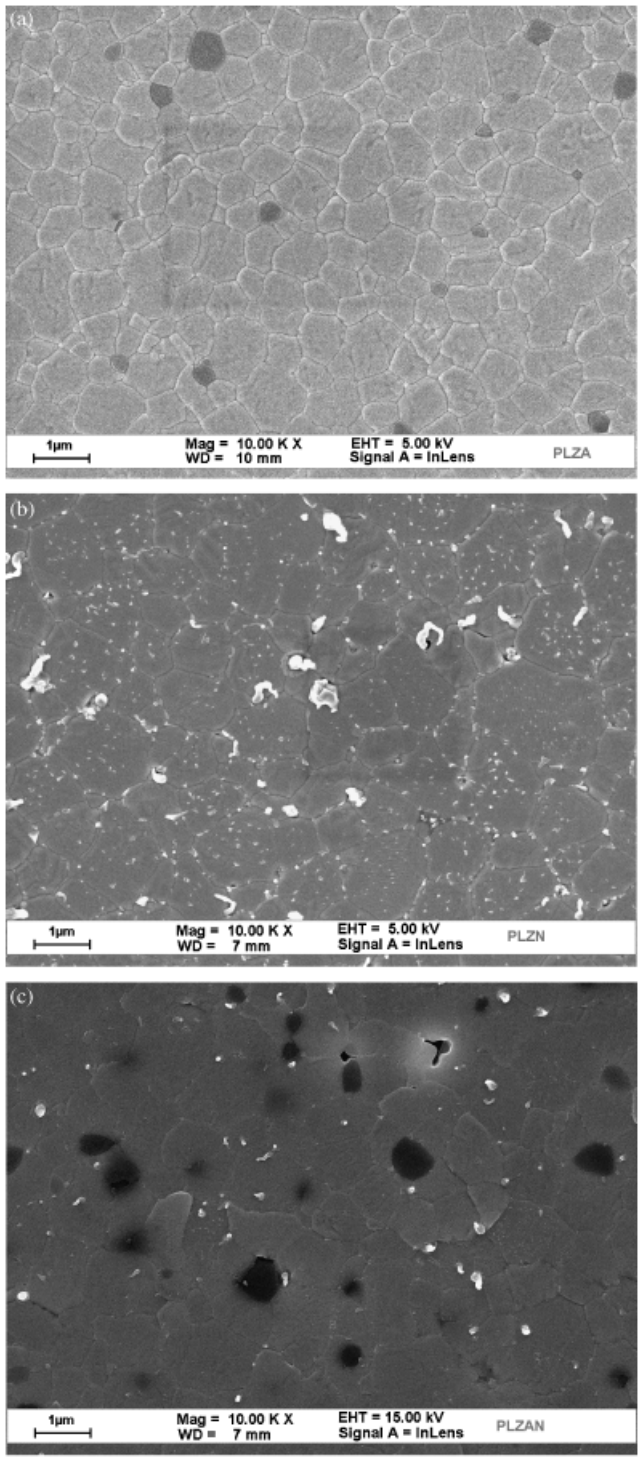

Fig. 2. Typical micrographs of (a) ZrO_2/Al_2O_3, (b) ZrO_2/Ni, and (c) ZrO_2/(Ni+Al_2O_3) composites after sintering at 1600°C for 1 h.

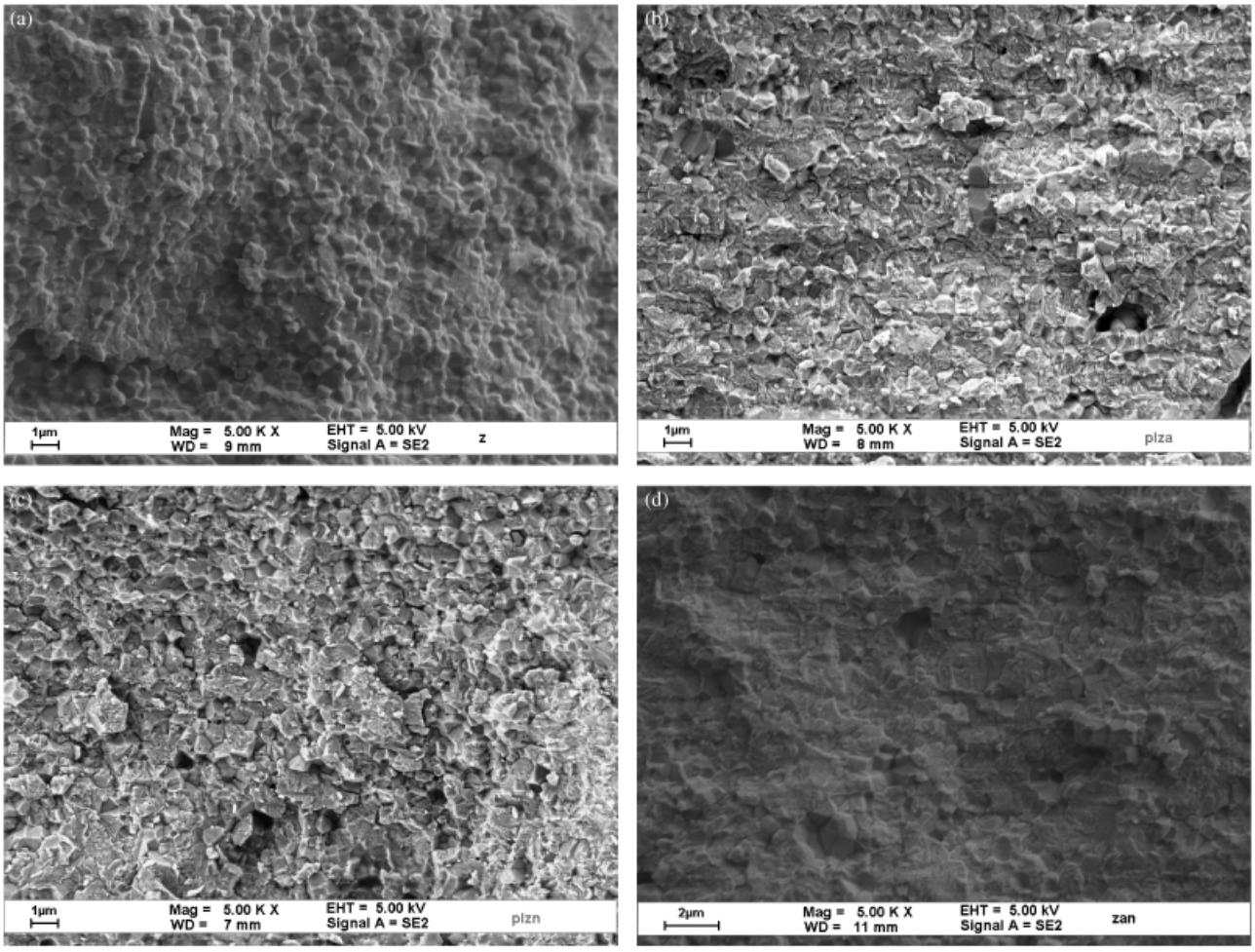

Fig. 3. Fracture surfaces of (a) ZrO_2, (b) ZrO_2/Al_2O_3, (c) ZrO_2/Ni, and (d) $ZrO_2/(Ni+Al_2O_3)$ specimens.

size of ZrO_2 grains in the composites was slightly larger than that of monolithic ZrO_2 (see Table I). The fracture surfaces of the specimens are shown in Fig. 3. The fracture mode of monolithic ZrO_2 is predominantly intergranular. A higher extent of transgranular fracture can be found in the ZrO_2/Al_2O_3, ZrO_2/Ni, and $ZrO_2/(Ni+Al_2O_3)$ composites.

The elastic modulus of the ZrO_2/Al_2O_3, ZrO_2/Ni, and $ZrO_2/(Ni+Al_2O_3)$ composites was slightly higher than that of monolithic ZrO_2 (see Table II). The strength of the composites, especially the Ni-containing ones, was higher than that of the monolithic ZrO_2 specimen. The addition of a small amount of Al_2O_3, Ni, or $Ni+Al_2O_3$, however, had little influence on the toughness of ZrO_2.

Figure 4 shows the magnetization curves of monolithic ZrO_2, ZrO_2/Ni, and $ZrO_2/(Ni+Al_2O_3)$ nanocomposites. Although the Ni-containing nanocomposites exhibit ferromagnetic characteristics, both the saturated magnetization and coercivity were small. The dielectric constant k at room temperature of the $ZrO_2/(Ni+Al_2O_3)$ nanocomposite was 33, which is slightly higher than that of monolithic ZrO_2 ($k = 25$).

Table II. Mechanical Properties of Monolithic ZrO_2, ZrO_2/Al_2O_3 Composite, and ZrO_2/Ni and $ZrO_2/(Ni+Al_2O_3)$ Nanocomposites

	Elastic modulus (GPa)	Strength (MPa)	Toughness ($MPam^{0.5}$)	Griffith flaw size (μm)
ZrO_2	193	666 ± 23	3.4	20
ZrO_2/Al_2O_3	206	978 ± 37	3.6	11
ZrO_2/Ni	217	1351 ± 37	3.4	5
$ZrO_2/(Ni+Al_2O_3)$	211	1187 ± 78	3.6	7

IV. Discussion

One previous study demonstrated that the addition of 20–40 vol% micrometer-sized Al_2O_3 particles prevented the coarsening of a ZrO_2 matrix.[6] The amount of Al_2O_3 used in the present study was much lower than 20 vol%. The addition of a small amount of Al_2O_3 particles increases both the final density and

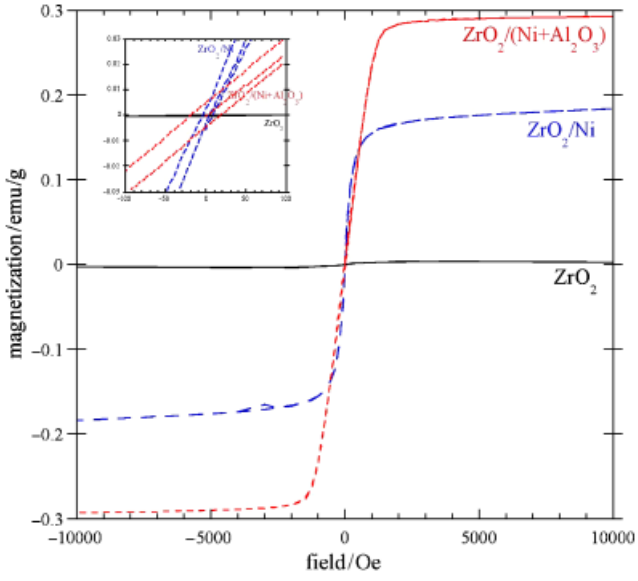

Fig. 4. Magnetization curves of monolithic ZrO_2, ZrO_2/Ni, and $ZrO_2/(Ni+ZrO_2)$ nanocomposites at room temperature.

the grain size. From previous studies on Al_2O_3/SiC nanocomposites, the SiC particles may act as a grinding medium to Al_2O_3 agglomerates during the milling stage.[13] The hardness of Al_2O_3 is higher than that of ZrO_2, and therefore, the Al_2O_3 particles may also act as a grinding medium in ZrO_2 agglomerates during turbo mixing. This is demonstrated by the fact that the fired density of the Al_2O_3/ZrO_2 composites is higher than that of Al_2O_3 (see Table I). A faster densification rate and less large pores in the green compact then lead to a larger grain size after sintering.

The strength of ZrO_2 is enhanced with Al_2O_3 inclusions. The Griffith flaw size c for the specimen can be estimated from the strength σ and toughness values K_{IC} with the following equation:

$$c = \left(\frac{K_C}{Y\sigma}\right)^2 \tag{1}$$

where Y is the stress intensity function of the crack. Assuming that the crack is half-penny shaped, $Y = 2/\sqrt{\pi}$. The critical flaw size is reduced with the addition of Al_2O_3 particles to the ZrO_2 matrix (see Table II), hence, the mechanical strength of ZrO_2 is improved.

The solution coating technique is a powerful method of introducing nanometer-sized particles into micrometer-sized particles, as demonstrated by many previous studies.[9,14] However, the amount of nanoparticles added may be limited by the availability of surface charge on the micrometer particles. The amount of surface charge on the ZrO_2 particles is low under the current experimental conditions, and, therefore, the amount of nanometer-sized Ni introduced onto the surface of the ZrO_2 particles is low: approximately 1 vol%. The dispersion of the ZrO_2 particles is aided by the presence of surface charges. The density of the Ni-containing composites is thus higher than that of the ZrO_2 specimen.

In the present study, many fine Ni particles were found within the ZrO_2 grains (see Fig. 2(b)), indicating that the fine Ni inclusions had a relatively small influence on the movement of ZrO_2 grain boundaries. A faster densification can lead to a larger grain size, and therefore, the size of ZrO_2 grains in the Ni-containing nanocomposites is larger than that in the monolithic ZrO_2. The critical flaw size is smaller in the Ni-containing nanocomposites (see Table II); hence, the mechanical strength is higher.

Apart from the increase in strength, the amount of transgranular fracture in the ZrO_2/Al_2O_3 composite is higher than that in the monolithic ZrO_2. This indicates that the strength of the grain boundary is increased. The addition of excess Al_2O_3 (above the solubility limit) can exert a scavenging effect on the ZrO_2 matrix,[15] namely, the Al_2O_3 inclusions can attract silica onto their surfaces, resulting in cleaner grain boundaries, which may subsequently lead to larger ZrO_2 grains in the ZrO_2/Al_2O_3 composite. Furthermore, cleaner grain boundaries can give rise to a higher grain boundary strength.

A change in fracture mode from intregranular to transgranular can be noticed for the Ni-containing nanocomposites. This phenomenon has also been reported for Al_2O_3/SiC nanocomposites.[13,16] The increase in grain boundary strength may have originated from: (1) crack deflection from grain boundary to grain by Ni particles and (2) change in local stresses because of the thermal expansion mismatch.[16] For the Al_2O_3/SiC nanocomposites, the mismatch in thermal expansion between the matrix and inclusion leads to the formation of radial compressive stress within the inclusions and tensile stress in the matrix. The presence of tensile stress in the matrix grains favors the deflection of crack from grain boundaries into the adjacent grains.

The change in fracture mode has not yet been documented for the Si_3N_4/SiC and Al_2O_3/Ni nanocomposites.[17,18] For these two systems, the thermal expansion of the inclusion is higher than that of the matrix, and therefore, the presence of residual stress may not underline the change in fracture mode. In the case of a ZrO_2/Ni system, the thermal expansion of ZrO_2 ($12 \times 10^{-6}\ K^{-1}$) is slightly lower than that of Ni ($13.3 \times 10^{-6}\ K^{-1}$). In a recent study on the ZrO_2/Ni composites,[14] a hard amorphous layer was observed around the Ni nanoparticles. Although the formation mechanism of this layer has not yet been investigated, the presence of such a hard layer may induce a crack path deflection.

One previous study demonstrated that adding NiO to the ZrO_2 matrix promoted a transformation from a *t*-phase to an *m*-phase.[19] The addition of NiO to ZrO_2 thus enhances the toughness of ZrO_2. Careful quantitative XRD analyses have been conducted on the fracture and ground surfaces. The ground surface was prepared by grinding the surface with a resin-bonded diamond wheel at a depth of 5 or 20 μm. No significant difference was noticed between the amount of *m*-phase in the monolithic ZrO_2 and that in the Ni-containing nanocomposites. Therefore, the toughness for the composites prepared in the present study is similar to that of monolithic ZrO_2 specimen (see Table II).

Metallic Ni is a ferromagnetic material. The addition of Ni particles conferred a ferromagnetic characteristic to the matrix ZrO_2. However, the saturated magnetization and coercivity of the ZrO_2/Ni and $ZrO_2/(Ni+Al_2O_3)$ nanocomposites were low (see Fig. 4). These values are lower than those reported previously by Kondo *et al.*[7] The Ni content in Kondo *et al.*'s nanocomposite is 1–2 vol%, and the size was 100–200 nm, which is larger than the Ni inclusions in the present study. It is well-known that ferromagnetic properties depend strongly on the particle size.[20] A particle with a size close to the size of a single domain exhibits excellent ferromagnetic behavior. This implies that the Ni inclusions prepared in the present study do not reach the critical size.

The introduction of metallic particles into an insulator reduces the size of effective electric field.[8] However, the amount of Ni particles was much lower than the percolation threshold, and therefore, the dielectric constant remained low. This is also reflected by a high electrical resistivity ($>10^{12}\ \Omega \cdot cm$).

V. Conclusions

The addition of both Ni and Al_2O_3 inclusions significantly enhances the strength of ZrO_2. The strength increase was due to a decrease in flaw size and not an increase in toughness, which may be a result of grain boundary strengthening. The addition of nanometer-Ni inclusions can transform ZrO_2 from a non-ferromagnetic to a ferromagnetic and ferroelectric material. Although the saturated magnetization, coercivity, and relative permittivity of the nanocomposite are relatively low, these properties can be improved by increasing the Ni content or the Ni particle size. The present study demonstrates the versatility and potential of the $ZrO_2/(Ni+Al_2O_3)$ nanocomposite.

Acknowledgments

The valuable comments of Prof. Jay Shieh and Mr. Shu-Ting Guo were very helpful.

References

[1]M. J. Lance, E. M. Vogel, L. A. Reith, and W. R. Cannon, "Low-Temperature Aging of Zirconia Ferrules for Optical Connectors," *J. Am. Ceram. Soc.*, **84** [11] 2731–3 (2001).

[2]M. Hirano, "Inhibition of Low Temperature Degradation of Tetragonal Zirconia Ceramics—A Review," *Br. Ceram. Trans. J.*, **91** [5] 139–47 (1992).

[3]K. Tsukuma, K. Ueda, and M. Shimada, "Strength and Fracture Toughness of Isostatically Hot-Pressed Composites of Al_2O_3 and Y_2O_3-PSZ," *J. Am. Ceram. Soc.*, **68** [1] c-4–5 (1985).

[4]W. C. Maskell, "Progress in the Development of Zirconia Gas Sensors," *Solid State Ionics*, **134** [1] 43–50 (2000).

[5]W. Z. Zhu and S. C. Deevi, "A Review on the Status of Anode Materials for Solid Oxide Fuel Cells," *Mater. Sci. Eng.*, **A362** [2] 228–39 (2003).

[6]S. Lopez-Esteban, J. F. Bartolome, and J. S. Moya, "Mechanical Performance of 3Y-TZP/Ni Composites: Tensile, Bending, and Uniaxial Fatigue Tests," *J. Mater. Res.*, **17** [7] 1592–600 (2002).

[7]H. Kondo, T. Sekino, Y.-H. Choa, T. Kusunose, T. Nakayama, M. Wada, T. Adachi, and K. Niihara, "Mechanical and Magnetic Properties of Nickel-Dispersed Tetragonal Zirconia Nano-Composites," *J. Nanosci. Nanotechnol.*, **2** [5] 485–90 (2002).

[8]C. Pecharroman, J. S. Bartolome, J. Requena, J. S. Moya, S. Deville, J. Chevalier, G. Fantozzi, and R. Torrecillas, "Percolative Mechanism of Aging in Zirconia-Containing Ceramics for Medical Applications," *Adv. Mater*., **15** [6] 507–11 (2003).

[9]W. H. Tuan, S. M. Liu, C. J. Ho, C. S. Lin, T. J. Yang, D. M. Zhang, Z. Y. Fu, and J. K. Guo, "Preparation of Al_2O_3–ZrO_2–Ni Nanocomposite by Pulse Electric Current Sintering and Pressureless Sintering," *J. Eur. Ceram. Soc*., **25** [13] 3125–33 (2005).

[10]B. D. Cullity, *Element of X-ray Diffraction*, 2nd edition, p. 101. Addison-Wesley Publ. Co. Inc., Reading, MA, 1978.

[11]P. A. Evans, R. Stevens, and J. P. Binner, "Quantitative X-Ray Diffraction Analysis of Polymorphic Mixes of Pure Zirconia," *Br. Ceram. Trans. J*., **84** [1] 39–43 (1984).

[12]B. R. Lawn, A. G. Evans, and D. B. Marshall, "Elastic/Plastic Indentation Damage in Ceramics: The Median/Radial Crack Systems," *J. Am. Ceram. Soc*., **63** [3] 574–9 (1984).

[13]J. Zhao, L. C. Stearns, M. P. Harmer, H. M. Chan, G. A. Miller, and R. E. Cook, "Mechanical Behavior of Alumina-Silicon Carbide Nanocomposites," *J. Am. Ceram. Soc*., **76** [2] 503–10 (1993).

[14]C. Pecharroman, F. Esteban-Betegon, J. F. Bartolome, G. Richter, and J. S. Moya, "Theoretical Model of Hardening in Zirconia-Nickel Nanoparticle Composites," *Nano Letters*, **4** [4] 747–51 (2004).

[15]X. Guo, "Role of Alumina in Zirconia for Functional Applications," *J. Am. Ceram. Soc*., **86** [11] 1867–73 (2003).

[16]M. Sternitzke, "Review: Structural Ceramic Nanocomposites," *J. Eur. Ceram. Soc*., **17** [5] 1061–82 (1997).

[17]T. Hirano and K. Niihara, "Microstructure and Mechanical Properties of Si_3N_4/SiC Composites," *Mater. Lett*., **22** [2] 249–54 (1995).

[18]T. Sekino, T. Nakajima, S. Uedaand, and K. Niihara, "Reduction and Sintering of a Nickel–Dispersed-Alumina Composite and its Properties," *J. Am. Ceram. Soc*., **80** [5] 1139–48 (1997).

[19]H. Kondo, T. Sekino, T. Kusunose, T. Nakayama, Y. Yamamoto, M. Wada, T. Adachi, and K. Niihara, "Solid-Solution Effects of a Small Amount of Nickel Oxide Addition on Phase Stability and Mechanical Properties of Yttria-Stabilized Tetragonal Zirconia Polycrystals," *J. Am. Ceram. Soc*., **86** [3] 523–5 (2002).

[20]B. D. Cullity, *Introduction to Magnetic Materials*, p. 385–9. Addison-Wesley Publ. Co. Inc., Reading, MA, 1972. □